The Minimum Modulation Curve as a tool for specifying optical performance: application to surfaces with mid-spatial frequency errors

HAMIDREZA ARYAN, 1,2 GLENN D. BOREMAN, 1,2 AND THOMAS J. SULESKI 1,2*

Abstract: There are a variety of common situations in which specification of a one-dimensional modulation transfer function (MTF) or two orthogonal profiles of the 2D MTF are not adequate descriptions of the image quality performance of an optical system. These include systems with an asymmetric on-axis impulse response, systems with off-axis aberrations, systems with surfaces that include mid-spatial frequency errors, and freeform systems. In this paper, we develop the concept of the Minimum Modulation Curve (MMC). Starting with the two-dimensional MTF in polar form, the minimum MTF for any azimuth angle is plotted as a function of the radial spatial frequency. This can be presented in a familiar form similar to an MTF curve and is useful in the context of guaranteeing that a given MTF specification is met for any possible orientation of spatial frequencies in the image. In this way, an MMC may be of value in specifying the required performance of an optical system. We illustrate application of the MMC using profile data for surfaces with mid-spatial frequency errors.

© 2019 Optical Society of America under the terms of the OSA Open Access Publishing Agreement

1. Introduction

The MTF is a measure of system performance over its full spatial frequency range. The MTF provides an objective evaluation of a system's imaging contrast and is expressed as the ratio of contrast in the image to contrast in the object as a function of spatial frequency [1]. MTF specifications given to manufacturers are often based conceptually on the conventional 1D-MTF representation, which plots a particular cross section of the 2D MTF, since the 2D MTF is less convenient as a practical specification. However, plotting a cross section is an incomplete specification of performance if the system's MTF is not rotationally symmetric or if the MTF is not a separable function of x and y spatial frequencies. A means to specify performance is desirable, which would guarantee that the desired performance is met regardless of the orientation of spatial frequencies in the image. In this paper, we propose a performance specification that captures key information from the 2D-MTF and presents it in the more familiar 1D format [2].

A 2D MTF can be defined as the magnitude of the Fourier transform of the 2D point spread function (PSF):

$$MTF(f_x, f_y) = \left| \int_{-\infty}^{\infty} PSF(x, y) e^{-j2\pi(xf_x + yf_y)} dxdy \right|, \tag{1}$$

Where f_x and f_y denote the spatial frequencies associated with the x and y spatial variables. The 2D MTF can be conveniently described in polar coordinates by means of the change of variables $\rho = (f_x^2 + f_y^2)^{1/2}$ and $\phi = \tan^{-1}(f_y/f_x)$, yielding $MTF(\rho, \phi)$. The radial spatial frequency ρ is represented as the radial distance from the center of the 2D polar plot and the azimuth angle ϕ corresponds to the angle measured from the f_x axis.

¹Department of Physics and Optical Science, University of North Carolina at Charlotte, Charlotte, NC 28223, USA

²Center for Freeform Optics, University of North Carolina at Charlotte, Charlotte, NC 28223, USA *tsuleski@uncc.edu

Section 2 introduces the concept of the Minimum Modulation Curve and its relationship to the 2D MTF. Section 3 illustrates the MMC representation with some specific examples drawn from systems with mid-spatial frequency errors, and section 4 discusses the importance of this analysis approach and possible future investigations for systems with inherently asymmetric performance. We note that in this paper we focus on the MTF of the optical components in the system and do not consider impacts of sensors or detectors [3].

2. The minimum modulation curve

In developing a performance specification for an optical system, it is desirable to ensure that a certain minimum MTF is present at the spatial frequencies of interest as a pass/fail criterion. Thus, we choose to determine the minimum modulation values, independent of orientation, to conform with the normal practice of setting acceptance criteria for the MTF. Choosing the minimum modulation values may be pessimistic if the MTF requirement is needed only for a specific orientation with a well-defined axis, but this is not the case for applications for which the relative orientation of the object and optical components are not well known or can vary.

Toward this end, we present the concept of the Minimum Modulation Curve (MMC), which conveniently summarizes the information contained within the 2D-MTF in the familiar form of a 1D plot, and which is suitable as a performance specification. Starting with the 2D MTF expressed in polar coordinates $MTF(\rho, \phi)$, we evaluate the MTF for all values of the azimuth angle for a given value of radial spatial frequency. The minimum MTF value at that ρ for any value of ϕ becomes the MMC value for that ρ :

$$MMC(\rho) = \min_{\phi \in [0, 2\pi]} \left\{ MTF(\rho, \phi) \right\},\tag{2}$$

as schematically illustrated in Fig. 1. The anisotropic MTF arising from a sample ZEMAX design file for a Cooke triplet with 40-degree field, at a wavelength of $\lambda = 650$ nm and off-axis field angle of 20°, is used as an example. The MMC for this case is shown in Fig. 2(a).

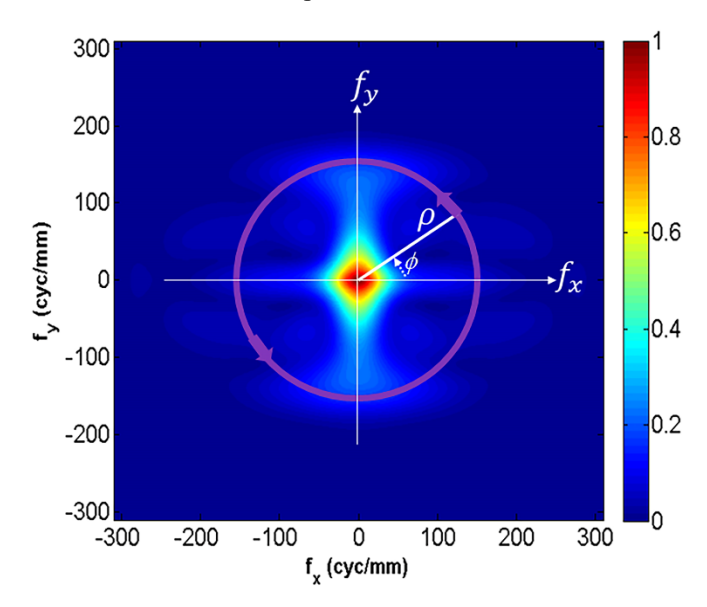


Fig. 1. Illustrating the methodology of extracting data for each spatial frequency from a general 2D-MTF. The minimum value around each circle is extracted to generate the MMC for a given value of radial spatial frequency ρ.

It is also of interest to calculate the standard deviation of MTF values $\sigma_{MTF}(\rho)$ for each value of ρ , assuming N values of azimuth angle ϕ :

$$\sigma_{MTF}(\rho) = \sqrt{\frac{\sum_{n=1}^{N} \left[MTF(\rho, \phi_n) - \frac{\sum_{n=1}^{N} MTF(\rho, \phi_n)}{N} \right]^2}{N}},$$
(3)

resulting in the MTF standard deviation plot as illustrated in Fig. 2(b). The MMC plot thus shows the minimum MTF for each frequency, considering all possible azimuth directions. The 1D nature of the plot facilitates a convenient comparison of measured data with a performance specification. In addition, the plot of MTF standard deviation $\sigma_{MTF}(\rho)$ can be used to identify the spatial frequencies that are most sensitive to anisotropy.

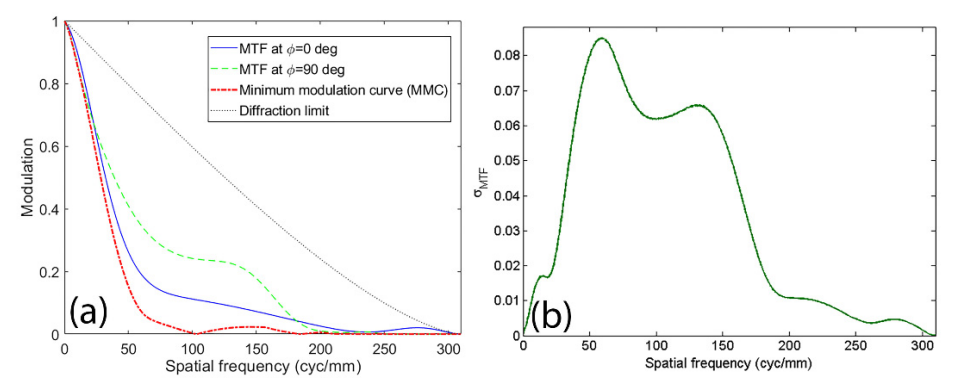


Fig. 2. With reference to the 2D MTF in Fig. 1(a), the minimum modulation curve (dash dot red) and horizontal MTF cross section (blue), (b) MTF standard deviation at each radial spatial frequency.

With the MMC and $\sigma_{MTF}(\rho)$ thus defined, we now consider optical components with residual mid-spatial frequency surface errors to illustrate the application of this concept.

3. Mid-spatial frequency errors and performance specification

Mid-spatial frequency (MSF) surface errors are common drawbacks of deterministic subaperture fabrication techniques [4-11]. The classic works for characterizing the impact of MSF errors on optical system performance generally assume that these errors are small and randomly distributed. Early studies on the impact of sub-aperture fabrication tool errors date back to evaluation of surface quality of diamond turned optics by Church and Zavada in 1975 [12]. However, their statistical approach requires that perturbations are small, and errors are random with no structured spatial frequencies in the Power Spectral Density (PSD) [13]. Marioge and Slansky considered the impacts of structured rotationally periodic waviness on image quality in 1983 [14]. More recently, Tamkin [15,16] has considered impacts of structured MSF errors on the Modulation Transfer Function (MTF). While high-spatialfrequency errors are often random in distribution and scatter the light at large angles, midspatial-frequency errors are far more structured and diffract the light at angles small enough to directly illuminate the image plane [17]. The distribution of this illumination depends on the structure of the errors on the surface, which in turn depends on the choice of fabrication technique. Typical MSF errors resulting from sub-aperture fabrication methods are not symmetric over the aperture, providing a suitable illustration for the presented analysis tools. It is important to keep in mind that different light distributions outside the main peak of the PSF will in result in different image quality performance. To illustrate this point, we assume two MSF errors with the same surface root mean squared (RMS) error values (82 nm) but different anisotropies. Figure 3 shows two diamond machined surfaces (turned and milled) synthesized in MATLAB using the same fabrication parameters: a tool-tip radius of 1 mm

and $\Lambda=40~\mu m$, where Λ represents feed/rev for turning and step-over for milling. A sinusoidal error of 1 cycle/mm with 150 nm peak to valley was added to the resulting 'cusp-shaped' tool errors to approximate thermal drift effects from the tool chiller during manufacturing.

Grating-like sinusoidal and cusp textures, such as those in Fig. 3, diffract the incident light which directly affects the system's performance. We assume a 4-mm diameter f/25 PMMA (n = 1.4934) lens at the aperture stop at wavelength $\lambda = 0.532~\mu m$ and perform a Rayleigh-Sommerfeld diffraction simulation to compare the impacts of these errors on performance.

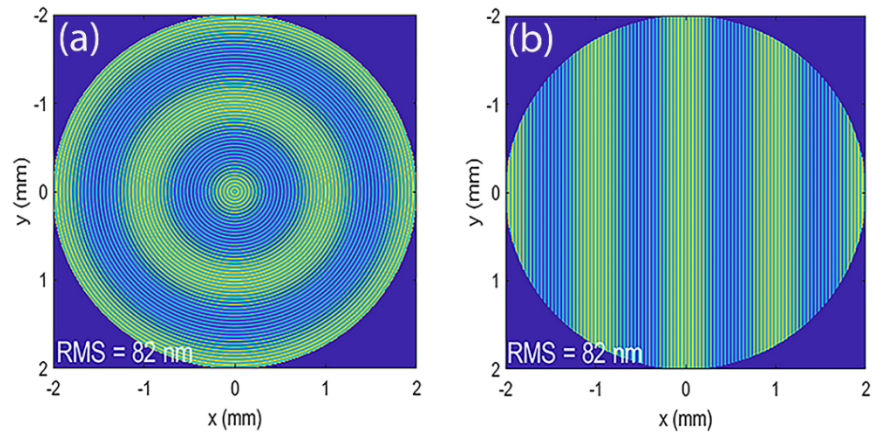


Fig. 3. Two diamond machined surfaces with the same fabrication parameters; Diamond tool cusp errors: a tool-tip radius of 1 mm and $\Lambda=40~\mu m$; Sinusoidal error of 1 cycle/mm with peak to valley (PV) of 150 nm to represent thermal errors. (a) Diamond turned. (b) Diamond milled.

Figure 4 compares the simulated PSFs for a perfect lens with no surface errors to lenses with the errors shown in Fig. 1. The PSF for the perfect lens has the typical Airy disk pattern. Diffraction from the rotationally symmetric grating pattern of the turned case appears as a symmetrical irradiance distribution in rings around the main peak, while the PSF corresponding to the milled case contains localized irradiance peaks in the horizontal direction. In other words, the turned pattern diffracts the light equally in all directions while the milled pattern diffracts in the horizontal direction, parallel to the grating vector.

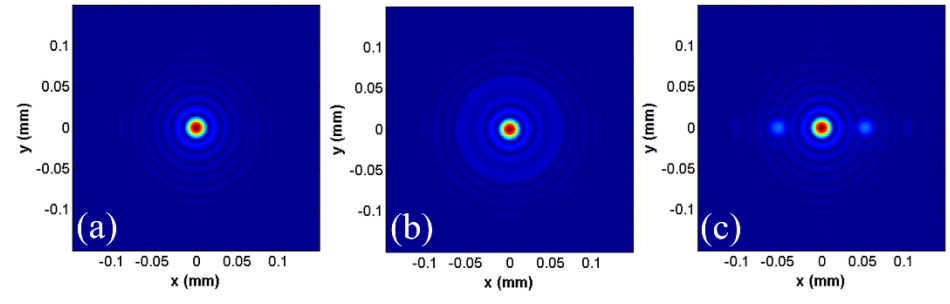


Fig. 4. Rayleigh-Sommerfeld simulations of PSF for the above examples for the (a) perfect lens, (b) diamond turned lens, (c) diamond milled lens.

The impacts of anisotropic MSF errors on optical performance are not well-understood or well-quantified because standard characterization methods are not able to sufficiently capture these impacts. This has led to problems in surface specification and setting acceptance criteria for testing purposes as well. Any surface specification method should show connections to optical performance, and without the right performance characterization method this problem will not be solved. Therefore, it is necessary to address this issue. The Strehl ratio and encircled energy radius have previously been considered as optical performance metrics for

surfaces with MSF errors [8,18,19]. Therefore, we first briefly consider these two metrics with respect to anisotropic MSF errors before considering the MTF and the MMC.

Strehl ratio (*SR*) is a commonly used single-number performance metric, defined as the ratio of on-axis intensity at the image plane for an aberrated system to that of a diffraction limited system [20]. For small wavefront variances, the Maréchal approximation [21] can be used to calculate the SR as:

$$SR = \exp[-(k\Delta n\,\sigma)^2],\tag{4}$$

Where $k = 2\pi/\lambda$, Δn is the difference between refractive indices of the lens and the surrounding medium, and σ is the surface RMS error. Since by definition the wavefront variance and surface RMS error are not sensitive to the shape of distribution of data over their spatial frequency content, the Strehl ratio is not able to distinguish between two wavefront variances with similar values but different shapes [8,22]. Rayleigh-Sommerfeld simulations result in SR = 0.8 for both cases, which agrees with prediction based on Eq. (4), and illustrates the inability to distinguish between the different performance impacts of these two surface errors using Strehl ratio.

Encircled energy radius (EER) is another common performance metric, defined as the radius of a circle with a certain amount of energy (typically 83%) centered on the PSF centroid [23]. Rayleigh-Sommerfeld simulations show an 83% encircled energy radius of ~0.05 mm for both cases in Fig. 1. Thus, neither Strehl ratio nor encircled energy are sufficient to distinguish between the impacts of the two surface errors illustrated in Fig. 1.

We now make use of Eq. (1) to calculate the 2D MTF from the three PSFs shown in Fig. 4. Unlike the results discussed above for *SR* and EER, the impacts of the different MSF error symmetries from Fig. 1 are clearly shown by the 2D MTFs in Fig. 5. We note that the 2D MTF also contains the Strehl ratio information if one integrates the volume under the 2D MTF [1,20]. Thus, the 2D MTF is a powerful tool to quantify the performance of an optical component with anisotropic performance characteristics. However, extracting key information from the 2D MTF and putting it in a one-dimensional form would make it more convenient as a means for performance specification.

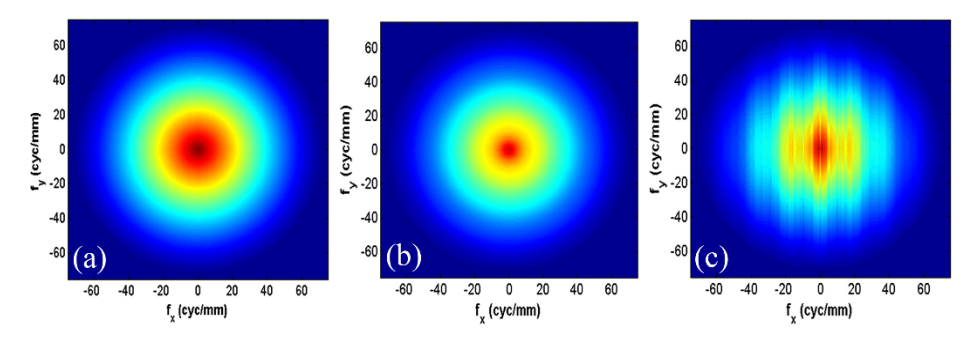


Fig. 5. 2D-MTF simulations for the (a) perfect lens, (b) diamond turned lens, (c) diamond milled lens. Red color represents 1 and blue color represents 0 modulation in these figures.

It is common to plot 1D horizontal and/or vertical cross sections of the 2D-MTF to represent the system MTF. However, a standard cross section of MTF is not an accurate representation when the MTF lacks rotational symmetry. Figure 6 compares the horizontal and vertical cross section of the 2D MTF from Fig. 5(c). Notice that the horizontal cross section indicates many MTF oscillations while a vertical cross section is smooth and approximately diffraction limited.

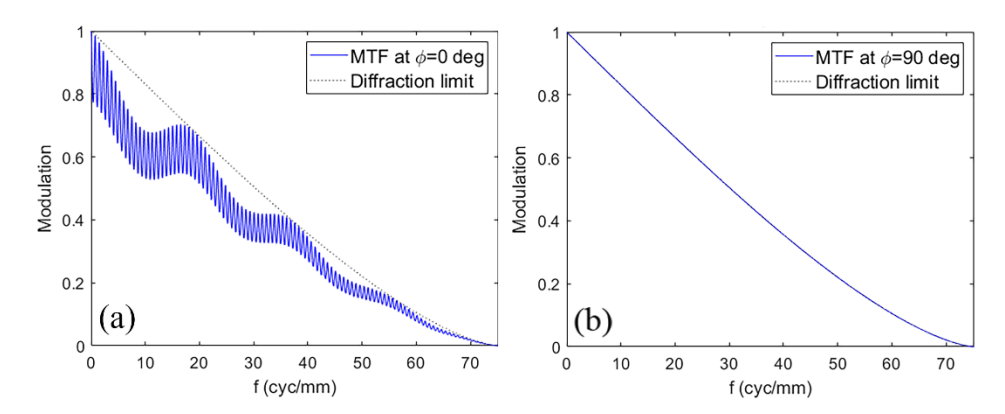


Fig. 6. Comparing (a) horizontal and (b) vertical cross section of the 2D-MTF for the diamond milled case from Fig. 3(b).

The high frequency oscillations in Fig. 6(a) are a result of the diamond 'cusp' errors on the surface [8,11]. In practice these oscillations will be minimal with a small machining stepover and corresponding small PV of the surface cusp error. In this example, we intentionally synthesized surfaces with a large stepover and PV to illustrate their impact in the MMC calculation.

We now apply the techniques described in Section 2 to determine the MMC and MTF standard deviation at each radial spatial frequency. The results are shown in Fig. 7.

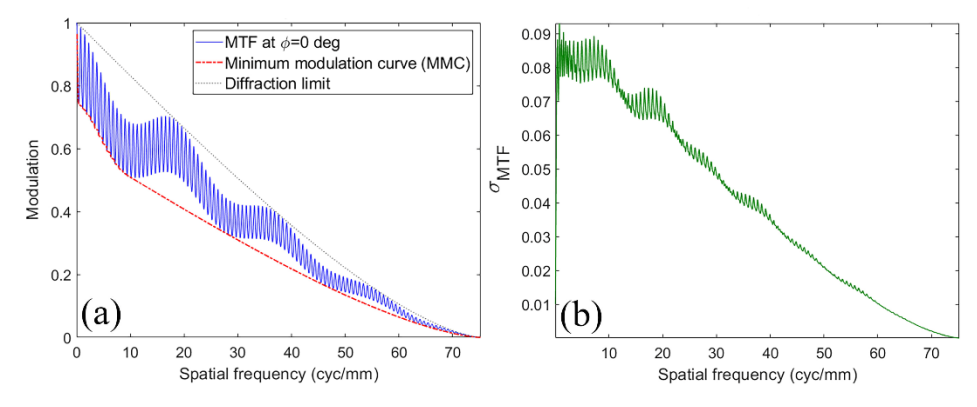


Fig. 7. With reference to the 2D MTF in Fig. 5(c). (a) the minimum modulation curve (dash dot red) and horizontal MTF cross section (solid blue), (b) MTF standard deviation at each radial spatial frequency.

We note that the MMC simplifies the oscillations on the 1D MTF in Fig. 7(a) by just presenting the minimum values, regardless of orientation. Also, the MTF standard deviation plot indicates that MTF varies more at low spatial frequencies, with an overall decline for higher frequencies. These tools may be useful to include in software packages for tolerancing purposes.

Rotationally asymmetric MTFs are also common when dealing with measured surface errors. As a demonstration, we consider an experimental surface error of the form shown in Fig. 8(a) applied to the surface of a calcium fluoride (n = 1.5576) f/10 lens in the deep ultraviolet region (λ = 157 nm). Figure 8(b) illustrates the 2D MTF for this system. In Fig. 8(c), the MMC plot indicates that, due to the anisotropy of the surface error, the actual optical performance would be worse than predicted by standard 1D-MTF cross sections. The MTF standard deviation plot in Fig. 8(d) shows the maximum MTF variations occur at approximately one-third of the lens cutoff frequency.

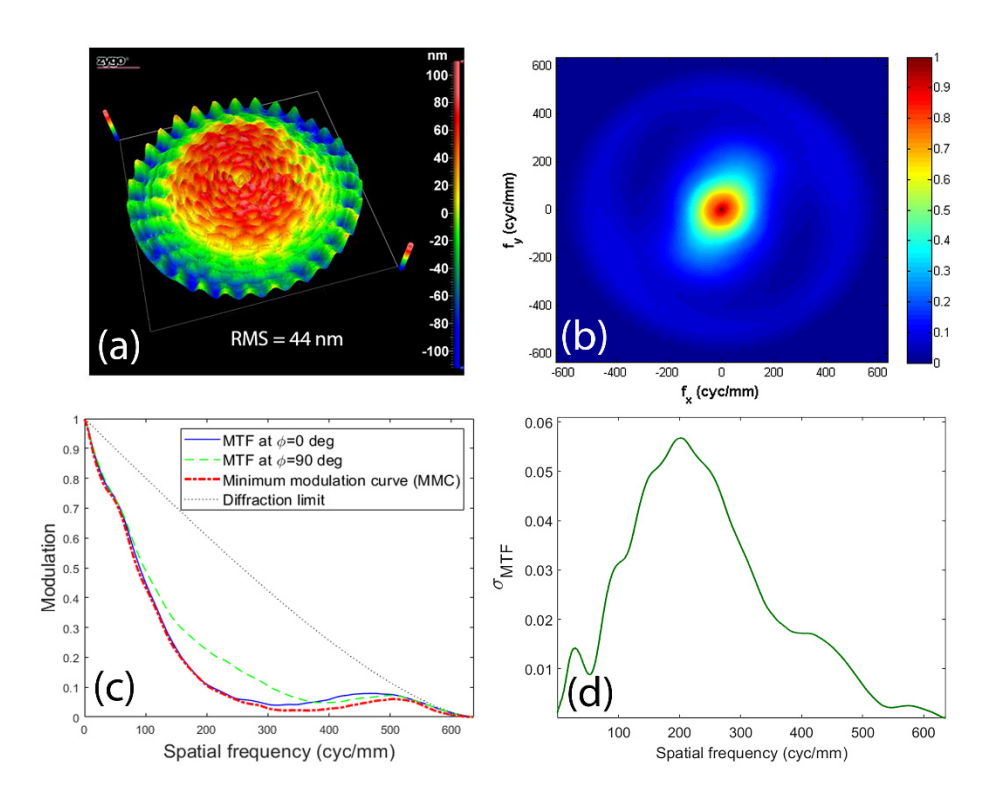


Fig. 8. (a) Measured surface error with RMS of 44 nm over a 127 mm clear aperture. (b) Simulated on-axis 2D MTF for a lens with this surface error. (c) Comparing MMC (dash dot red) with horizontal cross section of MTF at $\phi = 0^{\circ}$ (solid blue) and $\phi = 90^{\circ}$ (dash green). (d) MTF standard deviation at each radial spatial frequency.

4. Discussion and conclusion

We have presented a new analysis approach that identifies the minimum MTF value and its standard deviation at each radial spatial frequency, which is particularly useful for characterization and specification of system performance when PSFs and MTFs are not rotationally symmetric. In particular, the MMC presents information from the 2D MTF in an intuitive 1D format. It provides a straightforward way to represent the minimum MTF as a function of radial spatial frequency, considering all directions.

While we demonstrated the MMC for optical surfaces with mid-spatial frequency errors, the concepts presented in this paper may also be useful in other situations. For instance, in imaging applications, the final image is the weighted superposition of the system's PSF, which varies as a function of field angle, and the MTFs for off-axis field angles are often anisotropic. This is of particular importance for many modern optical systems; for instance, end users are sensitive to asymmetric image quality in digital single lens reflex (DSLR) and mirrorless camera lenses, as well as cell phone cameras [24].

Freeform optical systems also provide additional examples of PSFs and MTFs that are not rotationally symmetric. Many freeform systems have no single plane of symmetry and the performance metrics can no longer be assumed to be rotationally symmetric for such systems. Therefore, the performance evaluation must be considered over a full range of field points in two dimensions. Additionally, in augmented reality and virtual reality systems, near-eye display technology is used. In these applications, locations of the displayed image will move in response to movement of the user's head. In such situations, the user may be particularly sensitive to variations highlighted by σ_{MTF} .

Funding

National Science Foundation I/UCRC Center for Freeform Optics (IIP-1338877, IIP-1338898, IIP-1822049, and IIP-1822026).

Acknowledgments

Portions of this work were presented at the 2019 OSA Optical Design and Fabrication Congress in "Non-directional modulation transfer function for optical surfaces with asymmetric mid-spatial frequency errors." The authors acknowledge helpful discussions with Flemming Tinker from Aperture Optical Sciences (AOS), Dr. Matthew Davies, and Dr. Chris Evans from UNC Charlotte, and Dr. Miguel Alonso and Kevin Liang from the University of Rochester. We also would like to thank François Leprêtre from THALES for providing experimental data.

References

- 1. J. W. Goodman, Introduction to Fourier Optics, (Roberts and Company, 2005).
- H. Aryan, T. J. Suleski, "Non-directional modulation transfer function for optical surfaces with asymmetric midspatial frequency errors," in *Optical Design and Fabrication 2019 (Freeform, OFT), OSA Technical Digest* (online) (Optical Society of America, 2019), paper OT1A.2.
- O. Hadar, A. Dogariu, and G. D. Boreman, "Angular dependence of sampling modulation transfer function," Appl. Opt. 36(28), 7210–7216 (1997).
- R. Rhorer and C. Evans, "Fabrication of optics by diamond turning," in *Handbook of Optics, Third Edition Volume II: Design, Fabrication and Testing, Sources and Detectors, Radiometry and Photometry*, M. Bass, C. DeCusatis, J. Enoch, V. Lakshminarayanan, G. Li, C. Macdonald, V. Mahajan, and E. Van Stryland, eds. (McGraw-Hill, 2009), Chap. 10.
- 5. W. B. Lee, C. F. Cheung, and S. To, "Materials-induced vibration in single point diamond turning," in *Machining Dynamics*, K. Cheng, ed. (Springer, 2009), pp. 263–282.
- C. R. Dunn and D. D. Walker, "Pseudo-random tool paths for CNC sub-aperture polishing and other applications," Opt. Express 16(23), 18942–18949 (2008).
- 7. A. Sohn, L. Lamonds, and K. Garrard, "Modeling of Vibration in Single-Point Diamond Turning," in *Proceedings of the American Society of Precision Engineering* (ASPE, 2006), pp. 15–20.
- H. Aryan, K. Liang, M. A. Alonso, and T. J. Suleski, "Predictive models for the Strehl ratio of diamond-machined optics," Appl. Opt. 58(12), 3272–3276 (2019).
- 9. G. W. Forbes, "Never-ending struggles with mid-spatial frequencies," Proc. SPIE 9525, 95251B (2015).
- Z. Hosseinimakarem, H. Aryan, A. Davies, and C. Evans, "Considering a Zernike polynomial representation for spatial frequency content of optical surfaces," in *Imaging and Applied Optics 2015*, OSA Technical Digest (online) (Optical Society of America, 2015), paper FT2B.2.
- J. A. Shultz, H. Aryan, J. D. Owen, M. A. Davies, and T. J. Suleski, "Impacts of sub-aperture manufacturing techniques on the performance of freeform optics," in *Proceedings ASPE/ASPEN Spring Topical Meeting: Manufacture and Metrology of Structured and Freeform Surfaces for Functional Applications* (2017), paper 0061.
- E. L. Church and J. M. Zavada, "Residual surface roughness of diamond-turned optics," Appl. Opt. 14(8), 1788– 1795 (1975).
- J. C. Stover, "Roughness characterization of smooth machined surfaces by light scattering," Appl. Opt. 14(8), 1796–1802 (1975).
- 14. J. P. Marioge and S. Slansky, "Effect of figure and waviness on image quality," J. Opt. 14(4), 189-198 (1983).
- J. M. Tamkin, T. D. Milster, and W. Dallas, "Theory of modulation transfer function artifacts due to mid-spatial-frequency errors and its application to optical tolerancing," Appl. Opt. 49(25), 4825–4835 (2010).
- J. M. Tamkin, "A Study of Image Artifacts Caused by Structured Mid-spatial Frequency Fabrication Errors on Optical Surfaces," dissertation, The University of Arizona, (2010).
- 17. J. Filhaber, "Mid-spatial-frequency errors: the hidden culprit of poor optical performance," Laser Focus World 49(8), 32 (2013).
- M. A. Alonso and G. W. Forbes, "Strehl ratio as the Fourier transform of a probability density of error differences," Opt. Lett. 41(16), 3735–3738 (2016).
- F. Tinker and K. Xin, "Correlation of mid-spatial features to image performance in aspheric mirrors," Proc. SPIE 8837, 88370N (2013).
- 20. G. Boreman, Modulation Transfer Function in Optical and Electro-Optical Systems (SPIE Press, 2001).
- T. S. Ross, "Limitations and applicability of the Maréchal approximation," Appl. Opt. 48(10), 1812–1818 (2009).
- H. Aryan, C. J. Evans, and T. J. Suleski, "On the Use of ISO 10110-8 for Specification of Optical Surfaces with Mid-Spatial Frequency Errors," in *Optical Design and Fabrication 2017 (Freeform, IODC, OFT), OSA Technical Digest (online)* (Optical Society of America, 2017), paper OW4B.2.

- W. J. Smith, *Modern Optical Engineering, 3rd ed.* (McGraw-Hill, 2000), pp. 383–385.
 B. Dube, R. Cicala, A. Closz, and J. P. Rolland, "How good is your lens? Assessing performance with MTF full-field displays," Appl. Opt. 56(20), 5661–5667 (2017).